Dynamic control of β1 integrin adhesion by the plexinD1-sema3E axis

Young I. Choi[a,b,1], Jonathan S. Duke-Cohan[a,b,1], Wei Chen[c,d,e], Baoyu Liu[c,d,e], Jérémie Rossy[f,g], Thibault Tabarin[f,g], Lining Ju[c,d,e], Jingang Gui[a,b], Katharina Gaus[f,g], Cheng Zhu[c,d,e], and Ellis L. Reinherz[a,b,2]

[a]Laboratory of Immunobiology and Department of Medical Oncology, Dana-Farber Cancer Institute and [b]Department of Medicine, Harvard Medical School, Boston, MA 02115; [c]Coulter Department of Biomedical Engineering, [d]Woodruff School of Mechanical Engineering, and [e]Institute for Bioengineering and Bioscience, Georgia Institute of Technology, Atlanta, GA 30332; and [f]Centre for Vascular Research and [g]Australian Centre for Nanomedicine, University of New South Wales, Sydney, NSW 2052, Australia

Edited by Richard O. Hynes, Massachusetts Institute of Technology, Cambridge, MA, and approved November 18, 2013 (received for review July 29, 2013)

Plexins and semaphorins comprise a large family of receptor-ligand pairs controlling cell guidance in nervous, immune, and vascular systems. How plexin regulation of neurite outgrowth, lymphoid trafficking, and vascular endothelial cell branching is linked to integrin function, central to most directed movement, remains unclear. Here we show that on developing thymocytes, plexinD1 controls surface topology of nanometer-scaled β1 integrin adhesion domains *in cis*, whereas its ligation by sema3E *in trans* regulates individual β1 integrin catch bonds. Loss of plexinD1 expression reduces β1 integrin clustering, thereby diminishing avidity, whereas sema3E ligation shortens individual integrin bond lifetimes under force to reduce stability. Consequently, both decreased expression of plexinD1 during developmental progression and a thymic medulla-emanating sema3E gradient enhance thymocyte movement toward the medulla, thus enforcing the orchestrated lymphoid trafficking required for effective immune repertoire selection. Our results demonstrate plexin-tunable molecular features of integrin adhesion with broad implications for many cellular processes.

thymocyte development | mechanobiology | integrin activation | autoimmunity | central tolerance

It is well established that plexins and their semaphorin ligands regulate biological processes in multiple physiological domains including axon pathfinding (1, 2), angiogenesis (3), and immunity (4). Although plexins harbor potential for regulating small GTPases that mediate cytoskeletal remodeling, either through a direct cytoplasmic GTPase-activating protein (GAP) domain and Rac/Rho-GTPase binding domain or through sequestration of guanidine nucleotide exchange factor (GEF) proteins to the membrane-proximal cytoplasmic face, there is little consensus on plexin signaling pathways in a complex physiological context (5).

While studying the molecular interactions controlling mouse thymocyte development, we identified plexinD1 as a critical mediator for thymocytes destined to mature into T lymphocytes populating the mammalian immune system (6). *Plxnd1* encoding plexinD1 is transcriptionally regulated at a key intermediate stage of thymocyte development. Double-negative (DN) thymocytes lacking expression of CD4 and CD8 as well as plexinD1 differentiate in the thymic cortex into largely nondividing $CD4^+$ $CD8^+$ double-positive (DP) thymocytes that display surface αβ T-cell receptors (TCRs) and express plexinD1 (6). Despite being highly mobile (7), DP thymocytes remain sequestered in the cortex in frequent physical association with thymic epithelial cells (TECs), moving toward the thymic medulla via chemokine guidance only subsequent to TCR stimulation by self-derived peptide/MHC complexes (pMHC) that induce CD69 expression and support cell survival, i.e., positive selection (8, 9). $CD69^+$ DP cells differentiate further into $CD4^+CD8^-$ or $CD4^-CD8^+$ single-positive (SP) thymocytes, translocating to the thymic medulla to complete their maturation (10, 11). While traversing the thymus, immature αβ TCR^+ thymocytes that are strongly self-reactive with pMHC displayed on cortical and medullary TECs (cTECs and mTECs, respectively) are purged from the repertoire before peripheral exportation in a process termed negative selection (12–16).

In the absence of plexinD1, the majority of $CD69^+$ DP thymocytes remained cortically localized and, in contrast to the thymic trafficking of WT $CD69^+$ DP thymocytes, did not migrate toward the medulla (6). The specific expression of plexinD1 on cortical DP thymocytes led us to investigate the molecular regulation of adhesion by plexinD1 in thymocytes. Because thymocyte adhesion is integrin dependent (17), we focused on the regulation of developing thymocyte integrin function by plexinD1 and sema3E, its specific ligand. Here we show that plexinD1 controls thymocyte adhesion via a bimodal regulation of β1 integrin avidity where chemokine-induced migration is modulated by β1 integrin adhesion.

Results

Thymus Integrin-Ligand Expression. Following TCR stimulation through pMHC, activated $CD69^+$ DP thymocytes continue in a cortical to medullary direction, differentiating into CD4 or CD8 SP cells along the way. Because integrins play an essential role in hematopoietic cell migration, it is highly likely that the abnormal thymic localization of plexinD1 KO $CD69^+$ DP thymocytes results from aberrant integrin function. Although integrin and cognate ligand expression in thymus has been reported previously (18–20), a full characterization has not been undertaken for DP thymocytes, the cells that depend on plexinD1 for proper migration (6). We reasoned that retention of DP thymocytes in the cortex for several days during normal development implies

Significance

Cell-expressed integrins mediate adhesion with other cells and with extracellular matrix and are essential for embryonic development and for controlling leukocyte migration in later life. Integrin adhesion depends on conformational change leading to activation, although it remains unknown exactly how integrins alter their conformational state and adhesion in response to guidance cues. We show that the guidance molecule plexinD1 controls clustering of integrins in patches on the cell membrane and that the activation state of individual integrins in these patches can be switched off by binding of sema3E to plexinD1. Disruption of this pathway causes abnormal thymocyte adhesion regulation and migration during development, leading to autoimmune phenomena.

Author contributions: Y.I.C., J.S.D.-C., K.G., C.Z., and E.L.R. designed research; Y.I.C., J.S.D.-C., W.C., B.L., J.R., T.T., L.J., and J.G. performed research; Y.I.C., J.S.D.-C., J.R., K.G., C.Z., and E.L.R. analyzed data; and Y.I.C., J.S.D.-C., and E.L.R. wrote the paper.

The authors declare no conflict of interest.

This article is a PNAS Direct Submission.

[1]Y.I.C. and J.S.D.-C. contributed equally to this work.

[2]To whom correspondence should be addressed. E-mail: ellis_reinherz@dfci.harvard.edu.

This article contains supporting information online at www.pnas.org/lookup/suppl/doi:10.1073/pnas.1314209111/-/DCSupplemental.

IMMUNOLOGY

the presence of a cortical integrin ligand if DP thymocyte adhesion is mediated through integrins (21).

We therefore undertook a full examination of integrin ligand expression in the thymus, using the preferential distribution of keratin8 in the cortex together with strong medullary expression of MHC class II, ER-TR5, and UEA-1 to define the cortical and medullary regions (Fig. 1 and Fig. S1). We found that VCAM-1, a main ligand for α4β1 integrin and α4β7, was predominantly cortical in location, whereas laminin, the ligand for α6β1, was expressed throughout the thymus (Fig. 1). Integrin ligands with a strong medullary presence but minimal cortical expression included ICAM-1, the ligand for αLβ2, and osteopontin capable of interacting with α4β1, α4β7, and α5β1 (Fig. 1 and Fig. S1). Similarly, thrombospondin, which interacts with α4β1, was medullary localized, whereas mucosal addressin cell adhesion molecule 1 (MAdCAM1), a ligand for α4β7, was expressed on only a small population of medullary cells. Fibronectin (ligand for α4β1, α4β7, and α5β1) exhibited a strong medullary presence but was barely expressed in the cortex. Thus, VCAM-1 and laminin stand out as the primary thymic cortical ligands for thymocyte-expressed integrins, where VCAM-1 has potential to bind α4β1 and α4β7, and laminin isoforms bind α6β1 (Fig. S2*B*).

Because plexinD1 is barely expressed on DN1–DN4 thymocytes and highly expressed on DP thymocytes and subsequently down-regulated during the SP stage, we assessed expression of the putative integrin binding partners on thymocytes during the DN to DP to SP developmental transitions. We simultaneously assayed thymocyte subsets derived from animals where plexinD1 expression was conditionally knocked out during thymic development (D1CKO). The D1CKO cells lack any detectable plexinD1 (Fig. S2*D*). Examination of WT and D1CKO thymocytes revealed identical expression patterns of all known hematopoietically expressed integrin α and β chains throughout thymocyte development (Figs. S2–S4). Accordingly, any difference in integrin function between WT and D1CKO cells is unrelated to integrin expression levels. Analysis of integrin heterodimer display shows that at the DP stage, where plexinD1 expression is highly induced (6), the cells express individual integrin chains consistent with the expression of α4β1, α6β1, and αLβ2 (Fig. S2*B*). Because the ligand for αLβ2 is ICAM-1, which has a medullary location (Fig. 1), we focused exclusively on DP α4β1 and α6β1 binding to cortically localized VCAM-1 and laminin, respectively.

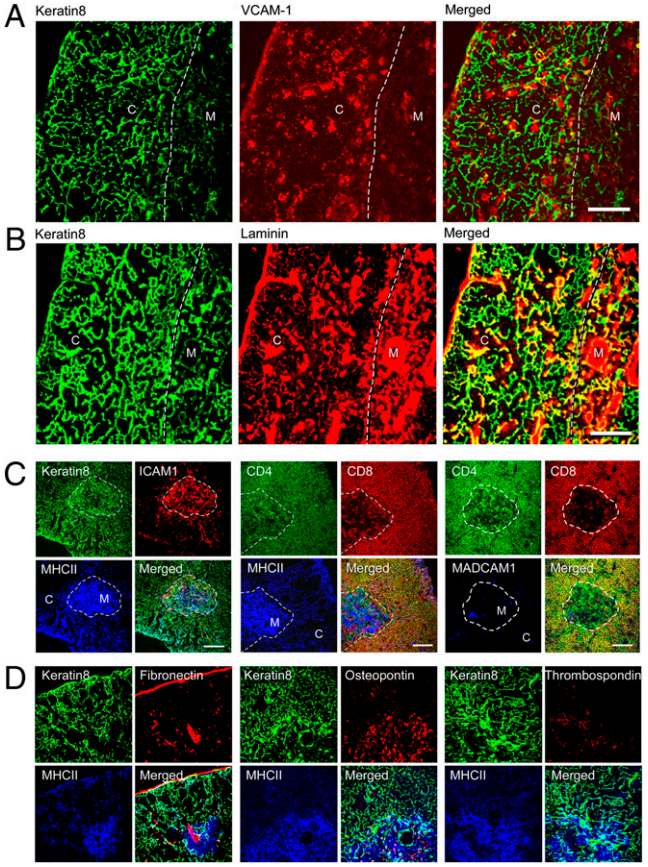

Fig. 1. Integrin ligand expression in the thymus. Confocal imaging of thymus cortex (C) and medulla (M) demonstrates (*A*) cortical location for VCAM-1 and (*B*) wide distribution of laminin. (Scale bar, 100 μm.) The dashed line in all images delineates the corticomedullary junction. Yellow color depicts merged green and red signals, white represents merged green, red, and blue signals, and cyan depicts merged green and blue signals. (*C* and *D*). ICAM-1, MHC class II, and osteopontin exhibit a medullary location. (Scale bar, 200 μm.) Note CD4 and CD8 colocalize on cortical DP cells.

PlexinD1 Regulates Dynamic Adhesion. Because WT and D1CKO α4β1 and α6β1 integrin expression is identical, we next examined whether their integrin activation state was comparable. Although reagents to reliably detect the mouse β1 integrin activation state are lacking, the SG31 mAb detects the metal ion-dependent adhesion site in an activated conformation of mouse α4 integrin chain (19). Binding of SG31 to the WT and D1CKO thymocyte subsets was identical, independent of preselection or postselection state marked by CD69 expression (Fig. S2 *D* and *E*). To assess integrin function more globally, we examined whether WT and D1CKO cells exhibited differential adhesion behavior on VCAM-1 or laminin-coated surfaces in a microfluidic chamber under flow conditions.

We observed strong adherence of WT thymocytes to VCAM-1, with >75% of the cells remaining adherent and stationary over 40 min and <13% of the cells detaching immediately on flow initiation (Fig. 2*A*, Movie S1, and Fig. S5). In contrast, the majority of D1CKO cells detached immediately. On laminin, the adherence of WT thymocytes was less strong and 39% detached immediately (Fig. 2*A*, Movie S2, and Fig. S6). Supporting the less robust adherence to laminin, fewer cells remained adherent; nearly 30% of the cells detached but then reattached leading to a stepwise rolling motion across the surface (Fig. S6). D1CKO cells detached from laminin as soon as flow was applied and the maximum velocity of the detaching/reattaching cells was increased (Fig. 2*A* and Fig. S7).

We then assessed the effect of sema3E addition on thymocyte adhesion by following the fraction of cells remaining adherent under flow conditions over time on VCAM-1–coated surfaces. Sema3E incubation resulted in the immediate detachment of >50% of the WT thymocytes that stably attach in the absence of sema3E (Fig. 2*B* and Movie S3). Supporting the argument that thymocyte α6β1 adhesion to laminin is less strong than α4β1 to VCAM-1, WT cells in the absence of sema3E detached when flow was applied but then reattached as they passed over the chamber surface, whereas cells in the presence of sema3E could not reattach (Fig. 2*B* and Movie S4). Thus, either the loss of plexinD1 or binding of its ligand sema3E reduced adhesion of α4β1 integrin to VCAM-1 or of α6β1 integrin to laminin. In contrast, sema3E had no effect on the adhesion dynamics of D1CKO cells, although, independent of sema3E, the D1CKO thymocytes exhibited cycles of detachment and reattachment in the direction of flow unlike adherent WT cells, which remained attached (Movies S5 and S6).

Examining responses to chemokines rather than a flow shear stress, cell migration in response to CXCL12 was observed on uncoated or VCAM-1–coated surfaces (Fig. 2*C* and Movie S7). Both WT and D1CKO cells moved rapidly toward the source, indicating no defect in cell migration machinery. On VCAM-1, however, a greater fraction of D1CKO cells was highly motile ($P < 0.05$). Mobility differences were even more pronounced between WT cells without and with sema3E addition with respect to mean velocity and by distance traveled (Fig. 2*C* and Movies S8 and S9; $P < 0.0001$). Hence, under flow conditions

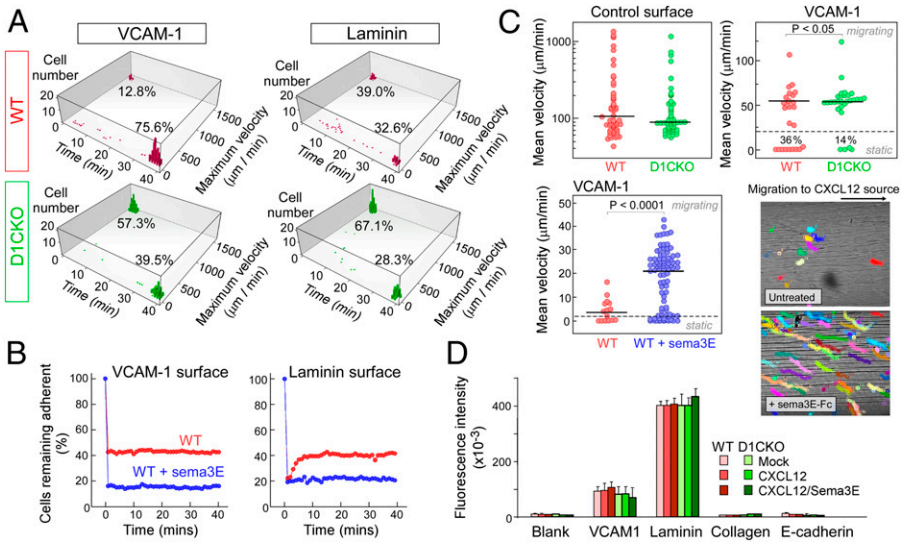

Fig. 2. PlexinD1/sema3E regulation of thymocyte dynamic adhesion. (*A*) Tracking of WT (red) and D1CKO (green) thymocytes under flow on VCAM-1– or laminin-coated surfaces. Nonadherent cells exhibited high maximum velocity at 0 min; adherent cells were immobile at 40 min. (*B*) Percentage of adherent untreated WT (red) and sema3E-treated WT thymocytes (blue) after induction of flow ($t = 0$). Initial cell numbers for WT: 659 on VCAM-1 and 480 on laminin; and for sema3E-treated WT: 454 on VCAM-1 and 145 on laminin. (*C*) Mean velocities of individual WT, D1CKO, and sema3E-treated WT cells on uncoated and VCAM-1–coated surfaces in response to a CXCL12 gradient originating on the right. Individual colored tracks of WT cells ± sema3E over a 30-min window (1,600-μm optical chamber width). (*D*) WT and D1CKO adhesion to various integrin ligands under static conditions. Adherence of intracellular fluorescent dye-labeled cells (10^6 per well) was quantified by emission at 530 nm after excitation at 485 nm. Mean ± SEM is shown.

or responding to chemokines, loss of plexinD1 or binding of sema3E to plexinD1 led to decreases in β1 integrin-mediated adhesion. No differences between WT and D1CKO cells, or between untreated WT and sema3E-treated WT cells, were detected using a static adhesion assay that measures specific integrin binding in the absence of force (Fig. 2*D*), indicating that static, stress-free conditions may not be suitable for assessing adhesion of motile cells.

PlexinD1 Constrains Surface β1 Integrin Topology. Our data imply that factors other than integrin expression are responsible for the functional differences in β1 integrin adhesion between WT and D1CKO thymocytes and between sema3E-treated and untreated WT thymocytes. Further, we found no difference between WT and D1CKO thymocytes in Rap1 signaling upstream of integrin activation, nor any difference in endocytic recycling of surface-expressed integrin, collectively suggesting that plexinD1 directly regulates β1 integrin expressed at the membrane (Fig. S8). We observed that plexinD1 colocalized with β1 integrins as well as with α4 and α6 integrins on the thymocyte surface, but not with β2 integrins (Fig. 3*A*), implying plexinD1 association with α4β1 and α6β1. This association was independent of stimulation by CXCL12, phorbol ester (PMA), or sema3E, implying proximity of plexinD1 and β1 integrins is constitutive (Fig. 3*B*).

Integrin avidity is also a function of the degree of clustering and integrin cluster density on the membrane surface (22, 23). We therefore used high-resolution direct stochastic optical reconstruction microscopy (dSTORM) to examine integrin organization at the molecular level (24). Individual β1 integrin molecules in a single cell were tightly clustered in WT thymocytes with few molecules residing outside clusters (Fig. 3*C*). In contrast, the D1CKO β1 integrins were less clustered, and a greater fraction of the integrin molecules was outside the clusters, confirmed by calculating the maximum degree of clustering relative to a random distribution [$Max\ L(r) - r$], and the percentage of integrins in clusters after applying a cluster threshold (Fig. 3*D*). β2 integrins were only minimally clustered reinforcing the confocal results (Fig. 3*A*). In the presence of sema3E, there was no change in the nanoscaled organization of β1 integrins on WT cells despite the functional alteration in adhesion (Fig. 2C) leading to a mechanistic distinction between thymocyte adhesion in the absence of plexinD1 and that after binding of sema3E to plexinD1. Supporting the observation above that sema3E has no effect on D1CKO thymocyte adhesion, sema3E also had no effect on surface β1 integrin nanoscale organization on D1CKO thymocytes (Fig. S9). Cluster morphology (Fig. 3*E*) was analyzed to extract information on area and circularity of these adhesive patches (Fig. S10) (25). As expected, β1 integrins on WT thymocytes formed a dense and circular cluster geometry that was independent of sema3E binding. In D1CKO cells, β1 clusters were significantly larger and less uniform, whereas the β2 clustering appeared almost amorphous (Fig. 3*E* and Fig. S10). The increased cluster area of β1 integrins in D1CKO cells and decreased integrin distribution into clusters (Fig. 3*D*) is evidence for loss of local nanoscale patch avidity under these conditions, contributing to reduced adhesion.

Sema3E Binding to PlexinD1 Controls β1 Integrin Catch Bonds. Because β1 surface geometry did not alter on sema3E binding, we postulated that sema3E must directly affect the β1 integrin heterodimer bond formation to VCAM-1 or laminin. We used a biomembrane force probe (BFP) to examine the biophysical parameters of thymocyte α4β1 binding to immobilized chimeric VCAM-1 fused to an Fc domain that provides correct orientation on a force-transducing bead (Fig. 4*A*) (26). We measured bond lifetime (reciprocal of dissociation rate) under force and molecular stiffness (Fig. 4 *B* and *C*), which reflects integrin conformation because bent integrins are less rigid (26). Analysis of bond lifetime revealed little difference between WT and D1CKO in control or sema3E-stimulated conditions under zero force (0pN; Fig. 4*B*). Given that adhesion under static conditions was identical but adhesion of mobile D1CKO or sema3E-incubated WT cells differed to that of untreated WT cells, we examined bond lifetimes under stress (10pN; Fig. 4*B*). WT cells formed bonds with long lifetimes that were shortened by sema3E incubation. D1CKO cells also expressed long bond lifetimes under stress but were not susceptible to sema3E.

Comparison of the molecular stiffness revealed that sema3E changed the integrin from an extended and active conformation to the bent and less active conformation but could not exert this effect on the D1CKO cells. Control activation experiments were performed in the presence of metal ions known to induce an extended conformation where sema3E clearly and significantly reduced molecular stiffness from this canonical state representing an extended integrin form (Fig. 4*C*). The generation of a stronger bond under force is consistent with the properties of catch bonds (27). Assay of the α4β1/VCAM-1 bond characteristics under a range of applied forces (Fig. 4*D*) demonstrated increasing bond stability up to 20 pN that then diminished as the applied force exceeded peak bond lifetime. In contrast, in the presence of sema3E bond lifetime was minimal, declining to negligible as force was applied. To further confirm the catch bond properties of the α4β1/VCAM-1 bond and its regulation by sema3E, we examined thymocyte rolling adherence and pause

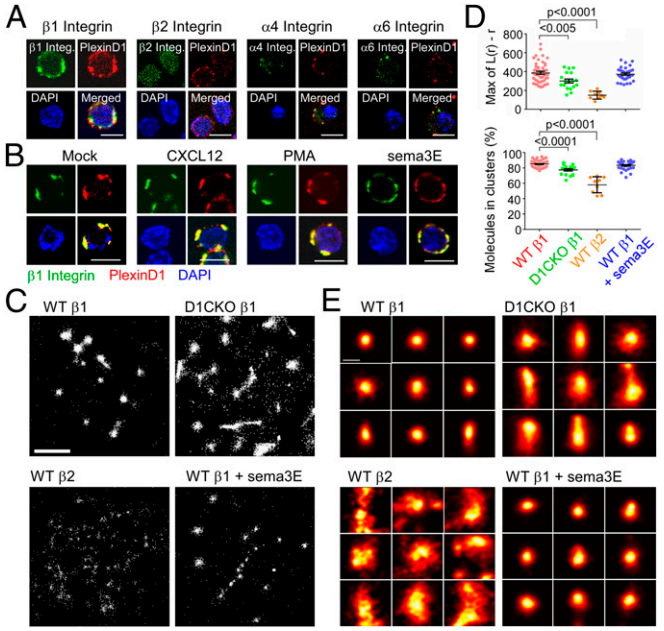

Fig. 3. β1 integrin surface topology is controlled by plexinD1 in thymocytes. (*A*) Colocalization of plexinD1 with β1, β2, α4, and α6 integrins detected by confocal microscopy. Merged red and green signals depicted as yellow. Blue signal represents nuclear DAPI staining. (*B*) Effect of indicated stimuli on colocalization of β1 integrin with plexinD1. For *A* and *B*, each image is representative of at least 60 cells imaged. (Scale bar, 5 μm.) (*C*) dSTORM image analysis of individual integrin molecules (single white dots) in a representative single cell of each indicated condition. Each panel is 4 μm square. (Scale bar, 1 μm.) (*D*) Degree of clustering [*Max L(r)-r*] and β1 and β2 integrin cluster distribution for the indicated cells and conditions. Each point represents a single cell analyzed. Mean ± SEM is depicted, and *P* is calculated from two-tailed Student *t* test. (*E*) Morphological analysis of representative β1and β2 integrin clusters (25). (Scale bar, 100 nm.)

time between consecutive rolling steps on a VCAM-1 coated surface in a flow chamber (Fig. 4*E* and Fig. S11) (28). Recapitulating the adherence characteristics under flow (Fig. 2*B*) and in response to chemokines (Fig. 2*C*), under increasing wall shear stress, WT thymocyte pause time increased, reached a maximum, and decreased (Fig. 4*E*), similarly to the single bond lifetime vs. force plot (Fig. 4*D*). In contrast, sema3E treatment significantly shortened the pause time (Fig. 4*E*) and reduced the number of rolling adherent cells on the VCAM-1 surface (Fig. S11), especially at wall shear stresses >0.5 dyn/cm^2. The qualitatively similar patterns between single-bond BFP data and multiple bond flow chamber data demonstrate that the α4β1/VCAM-1 catch bond and its regulation by sema3E are operative in integrin-mediated cell rolling in resistance to applied shear stress (28). Thus, plexinD1 exerts a bimodal effect on integrin avidity: first, by maintaining a dense clustered geometry of β1 integrins and, second, through interaction with its ligand sema3E, to abrogate β1 integrin catch bonds.

PlexinD1 Is Essential for Proper Thymic Selection Including Deletion of Autoreactive Specificities. This plexinD1 functional duality offers a mechanistic framework underlying the failure of most CD69$^+$ thymocytes to translocate toward the medulla in mice reconstituted with *Plxnd1*$^{-/-}$ fetal liver stem cells (6), with significant implications for repertoire selection. Specifically, as plexinD1 is down-regulated in positively selected CD69$^+$ DP thymocytes and their descendant immature SP thymocytes, surface β1 integrin clustering may be reduced, diminishing cell adhesion and permitting chemokine gradient-driven motility toward the medulla to complete the developmental process. We thus have refined our initial interpretation of plexinD1 regulation of chemokine migration (6) to propose that thymocyte tracking toward the medulla is impeded until β1 integrin adhesion is reduced following plexinD1 down-regulation and/or binding of sema3E emanating from the medulla. Loss of plexinD1 in conditional KO (D1CKO) mice should therefore have reduced topological constraint on nanoscale patches, diminishing integrin avidity. However, the β1 integrin catch bonds will remain intact and insensitive to the sema3E, thereby leading to increased cortical retention of CD69$^+$ thymocytes. The resultant reduced medullary migration of D1CKO thymocytes should impede negative selection, particularly that of CD4$^+$ SP thymocytes in the medulla, possibly leading to autoimmune phenomena (29–31).

To test this hypothesis, we examined negative selection in double transgenic OTII$^+$RIP-mOVA$^+$ B6 mice on WT vs. D1CKO backgrounds. In this system, OTII$^+$ Vβ5 TCR transgenic thymocytes move to the medulla and undergo negative selection on recognizing the OVA$_{323–339}$/I-A^b pMHC ligand derived from medullary expression of the RIP-mOVA$^+$ transgene (32, 33) (Fig. 5*A*). As expected, we found few OTII$^+$ CD4 SP thymocytes survived in the RIP-mOVA-expressing thymus (Fig. 5*B*; compare OTII$^+$ vs. OTII$^+$RIP-mOVA$^+$). In contrast, a significant number of OTII$^+$ CD4 SP thymocytes (Vβ5$^+$CD3ε$^+$) survived negative selection in the OTII$^+$RIP-mOVA$^+$ D1CKO mice (Fig. 5 *B* and *C*), comparable to that in the parental OTII$^+$ environment (Fig. 5*B*; compare OTII$^+$ vs. OTII$^+$RIP-mOVA$^+$ D1CKO). Despite an increase in the absolute number of D1CKO CD4 SP thymocytes surviving in comparison with WT CD4 SP thymocytes on the OTII$^+$RIP-mOVA$^+$ background (Fig. 5*C*), this difference was not observed between the respective DP populations. These data are consistent with impaired negative selection of immature OTII$^+$ D1CKO CD4 SP thymocytes rather than in the DP thymocytes themselves. Reflecting this, in peripheral lymphoid tissues such as lymph node and spleen, an increase in OTII TCR^{hi} CD4 SP cells was seen in RIP-mOVA$^+$ D1CKO mice but not in RIP-mOVA$^+$ WT mice (Fig. 5*D* and Fig. S12*A*).

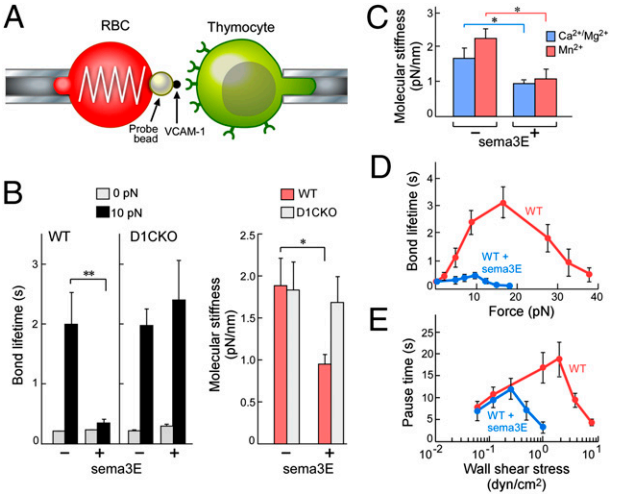

Fig. 4. Sema3E signaling through plexinD1 switches β1 integrin catch bonds. (*A*) BFP schematic: glass bead immobilized on erythrocyte is derivatized with VCAM-1 (black dot). α4β1 integrin depicted as green receptor on thymocyte. (*B*) Mean lifetime under zero force and under 10-pN force for WT and D1CKO cells ± sema3E ($n > 70$ for each condition). Effect of sema3E on molecular stiffness (active conformation) of α4β1 on WT and D1CKO cells ($n > 50$ for each condition). (*C*) Effect of sema3E on α4β1 integrin molecular stiffness of extended form induced by divalent metal ion binding. (*D*) Effect of sema3E on individual α4β1/VCAM-1 bond lifetimes on WT cells measured over a range of forces. (*E*) Effect of sema3E on WT rolling adherence (pause time intervals between rolling events) under increasing wall shear stress conditions. For all panels, mean ± SEM is shown; $*P < 0.05$; $**P < 0.025$.

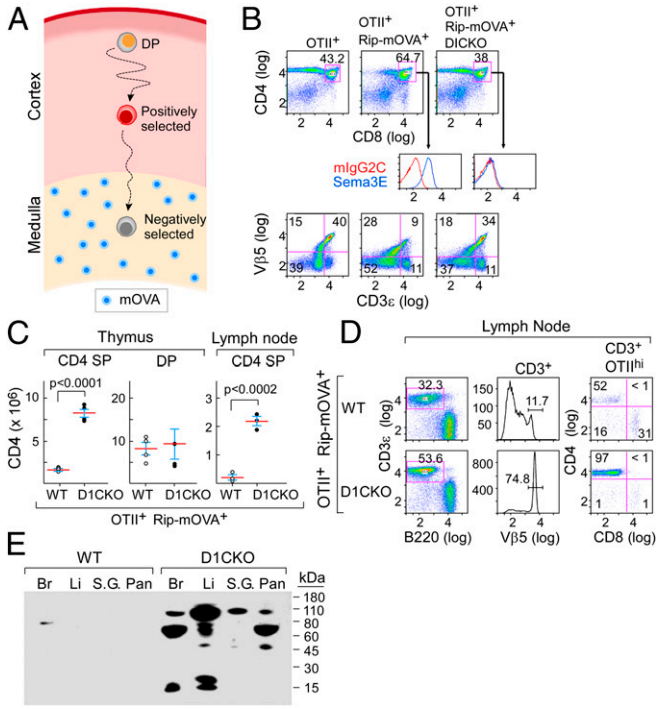

Fig. 5. Loss of thymocyte plexinD1 leads to defective negative selection. (*A*) Schematic of OTII$^+$*RIP-mOVA*$^+$ thymocyte selection. Ovalbumin expressed from the *Rip* promoter is degraded in the thymic medulla and presented on mTEC (blue) to positively selected thymocytes migrating from the cortex. For negative selection, OTII-TCR$^+$ thymocytes must move to the medulla. (*B*) Survival of CD4$^+$ SP OTII$^+$*RIP-mOVA*$^+$ D1CKO thymocytes in comparison with plexinD1-expressing OTII$^+$*RIP-mOVA*$^+$ thymocytes. (*Top*) CD4 vs. CD8 FACS dot plots on total thymocytes from indicated mouse strains. (*Middle*) Expression of plexinD1 enumerated by sema3E-Fc binding on gated DP thymocytes. (*Bottom*) Enumeration of mature Vβ5/CD3^{hi} thymocytes. (*C*) Survival of thymic and lymph node CD4 SP cells (absolute number per organ). Mean ± SD is shown. (*D*) Survival of OTII^{hi} lymph node T cells, gating on CD3ε then Vβ5 to observe CD4 subset. (*E*) Serum autoantibody reactivity with different tissues as detected by Western blotting (Br, brain; Li, liver; S.G., salivary gland; Pan, pancreas). Results of individual panels are representative of two to three independent experiments for each group of mice examined (where total $n > 8$).

It follows that if aberrant negative selection in OTII$^+$ RIP-mOVA$^+$ D1CKO mice is a consequence of a defect in directed migration of positively selected thymocytes, then no difference should be detected between OTII$^+$ D1CKO and OTII$^+$ WT mice on direct parenteral injection of $OVA_{323–339}$. Here, the TCR ligand will distribute throughout the entire thymus eliminating the requirement for thymocytes to migrate to the medulla and interact with this negatively selecting pMHC ligand (Fig. S12*B*). Consistent with this prediction, $OVA_{323–339}$ peptide injection induced an equivalent reduction of OTII$^+$ CD4 SP thymocytes in both WT and D1CKO mice (Fig. S12*C*).

Faulty deletion of a single autoreactive CD4 T-cell specificity was observed with the above TCR transgenic model. In nontransgenic B6 D1CKO mice, autoreactive T cells of a variety of specificities might similarly escape such selection. Using circulating autoantibodies as a proxy for CD4 T cell–linked autoimmunity, we tested serum autoantibody representation in D1CKO B6 and WT B6 mice by Western blotting against a panel of likely target tissues. Strong antitissue responses were observed (Fig. 5*E* and Fig. S12*D*) and confirmed by detection of anti–self-tissue antibodies in 9 of 12 D1CKO mice compared with 2 of 9 WT mice (Fig. S12*F*), with titers comparable to those observed in *Aire*$^{-/-}$ mice (31), a well-studied autoimmune model. Taken together, these data point to a key role for plexinD1 in directed thymocyte migration to foster negative selection and prevent T-cell autoreactivity.

Discussion

Our results demonstrate that sema3E binding to plexinD1 on DP thymocytes induces a loss of adhesion mediated by the β1 integrins α4β1 and α6β1 detaching from their thymic-expressed cellular and extracellular matrix ligands, VCAM-1 and laminin, respectively. The data show in explicit molecular terms how sema-binding initiates detachment, a component of repulsion. Remarkably, this regulatory function of plexinD1/sema3E is only manifest under motile thymocyte conditions, resulting in consequences for thymic immune repertoire selection. A recent study showing that plexinD1 is a regulator of germinal centers (GCs) and development of the humoral response implies that this physiology extends to B lymphocytes and their movement into the GC (34).

Although force often shortens bond lifetime (slip bonds), prolongation of bond lifetime (catch bonds) can occur as a consequence of conformational alteration in receptors. Since the initial demonstration of the P-selectin complex binding to PSGL-1 as a catch bond (35), these bonds have been demonstrated for integrins (27, 36), actomyosin (37), bacterial adhesion FimH (38), platelet glycoprotein Ibα (39), kinetochore protein (40), cadherin (41), and actin (42). Here we provide a definitive physiologic demonstration of catch bond regulation by a semaphorin signaling through a plexin. Despite reports of cross-talk between plexins, the cytoskeleton, and integrins, there is little evidence to support a specific signaling mechanism (43) or uniform conformational change on a semaphorin binding to a plexin (44, 45). Because the absence of plexinD1 does not release the activated conformation of β1 integrin but only the constraints on the tight nanoscale membrane clustering, we must conclude that the sema3E-independent function of plexinD1 does not affect the known intracellular dynamics of integrin activation. Those dynamics include integrin α and β chain cytoplasmic domain separation, association with talin, association with kindlin-3, and linkage of these proteins to the cytoskeleton stabilizing the activated integrin state (46, 47). We propose that plexinD1 per se functions as a scaffold to maintain β1 integrin in clusters. In contrast, sema3E binding initiates cytoskeletal remodeling via modulation of plexinD1-intrinsic or -associated GAP activity, breaking the cytoskeletal stabilization of the activated β1 integrin conformation (5).

The strong medullary expression of sema3E implies minimal influence of plexinD1 on medullary-localized thymocyte interactions mediated by β1 integrins. Likewise, the plexinD1-sema3E axis is unlikely to affect SP thymocyte-expressed αLβ2 integrin because the specific ligand ICAM-1 is medullary expressed. Moreover, the osteopontin-binding α4β7 integrin is expressed on CD8SP but not CD4SP thymocytes. Thus, CD8SP thymocyte regulation in the medulla will be distinct from that of CD4SP thymocytes, and regulation of catch bonds involving various additional integrin classes by other plexin/semaphorin family interactions cannot be excluded (27). We also propose that the same integrin regulatory functions observed herein for DP thymocytes also modulate neurite outgrowth and endothelial motility. Beyond physiologic functions, recent studies have shown that expression of sema3E and its receptor plexinD1 correlate with metastatic progression of human tumors through increasing invasiveness, transendothelial migration, and metastatic spread (48). Further, viruses create semaphorin mimics influencing host immune-related plexin activity; an example is that of the smallpox virus A39 sema7A mimic, which interacts with plexinC1 (49). These details of plexinD1-sema3E regulation of β1 integrin function will allow further elucidation of the molecular basis for plexin-semaphorin regulation of cellular repulsion or attraction.

Materials and Methods

Mice. Full details are provided in *SI Materials and Methods*.

Chemotaxis and Cell Motility Imaging. Thymocytes were allowed to adhere to uncoated, VCAM-1–, or laminin-coated microchannels and then exposed to flow or chemokine gradient with or without sema3E and imaged at 37 °C as described in *SI Materials and Methods*.

dSTORM Imaging and Analysis. For dSTORM images, thymocytes treated with or without Sema3E-Fc were stained with anti-β1 and anti-β2 antibodies coupled to biotin for 30 min on ice, labeled with Alexa Fluor 647-streptavidin for 30 min on ice, and, after washing, were plated onto poly-L-lysine–coated cover glasses by cytospin centrifugation and fixed in 4% (vol/vol) paraformaldehyde until analysis. Images were acquired in an oxygen scavenging buffer (24) on a total internal reflection fluorescence microscope (ELYRA; Zeiss) with a 100×, NA = 1.46 oil-immersion objective. For Alexafluor 647 dSTORM, imaging was performed at 30 mW with 633-nm laser illumination, and 0.1–1 mW of 488-nm laser light was used for conversion from the dark state. Fifteen thousand to 20,000 images were acquired per sample using a cooled, electron-multiplying charge-coupled device (EMCCD) camera (iXon DU-897D; Andor) with an exposure time of 30 ms. Image analysis was performed as described in *SI Materials and Methods*.

BFP Analysis. All experimental setup and detailed procedures have been previously described (26, 27). In brief, we assembled an ultrasensitive force probe by attaching a streptavidin-conjugated bead to the apex of a biotinylated RBC aspirated by a stationary micropipette (Fig. 4*A*). The streptavidin-coupled bead was first incubated with biotinylated goat-anti-mouse-Fc antibody followed by mouse VCAM-1-Fc. A thymocyte aspirated by a separate micropipette was driven by a piezoelectric translator (Physical Instruments) with subnanometer precision via a capacitive sensor feedback control (Fig. 4*A*). The probe bead and the target cell were aligned in a cell chamber filled with L-15 buffer plus 0.5% human serum albumin and observed under an inverted microscope (Axiovert 100; Zeiss, a 40×/NA 0.75 objective plus a 4× TV tube) through two cameras at room temperature. One camera (CCD100; DAGE-MTI) captured real-time images at 30 frames/s (fps). The other camera (GE680; Prosilica) had high speed (1,600 fps) when the images were limited to a 30-line strip across the bead, which allowed a custom image analysis LabView (National Instruments) program to track the bead position with a 3-nm (SD) displacement precision (Fig. S13). Further details are provided in *SI Materials and Methods*.

ACKNOWLEDGMENTS. We thank Maris Handley and Elizabeth Witten for technical assistance. This work was supported by National Institutes of Health Grants AI19807 (to E.L.R.), AI92378 (to Y.I.C.), and AI44902 (to C.Z.), the Australian Research Council (K.G.), and the National Health and Medical Research Council of Australia (J.R. and K.G.).

1. Kolodkin AL, Matthes DJ, Goodman CS (1993) The semaphorin genes encode a family of transmembrane and secreted growth cone guidance molecules. *Cell* 75(7): 1389–1399.
2. Tessier-Lavigne M, Goodman CS (1996) The molecular biology of axon guidance. *Science* 274(5290):1123–1133.
3. Sakurai A, Doçi CL, Gutkind JS (2012) Semaphorin signaling in angiogenesis, lymphangiogenesis and cancer. *Cell Res* 22(1):23–32.
4. Takamatsu H, Kumanogoh A (2012) Diverse roles for semaphorin-plexin signaling in the immune system. *Trends Immunol* 33(3):127–135.
5. Hota PK, Buck M (2012) Plexin structures are coming: Opportunities for multilevel investigations of semaphorin guidance receptors, their cell signaling mechanisms, and functions. *Cell Mol Life Sci* 69(22):3765–3805.
6. Choi YI, et al. (2008) PlexinD1 glycoprotein controls migration of positively selected thymocytes into the medulla. *Immunity* 29(6):888–898.
7. Yin X, et al. (2007) CCR7 expression in developing thymocytes is linked to the CD4 versus CD8 lineage decision. *J Immunol* 179(11):7358–7364.
8. Suzuki G, et al. (1998) Loss of SDF-1 receptor expression during positive selection in the thymus. *Int Immunol* 10(8):1049–1056.
9. Uehara S, Song K, Farber JM, Love PE (2002) Characterization of CCR9 expression and CCL25/thymus-expressed chemokine responsiveness during T cell development: CD3 (high)CD69+ thymocytes and gammadeltaTCR+ thymocytes preferentially respond to CCL25. *J Immunol* 168(1):134–142.
10. Davalos-Misslitz AC, Worbs T, Willenzon S, Bernhardt G, Förster R (2007) Impaired responsiveness to T-cell receptor stimulation and defective negative selection of thymocytes in CCR7-deficient mice. *Blood* 110(13):4351–4359.
11. Egerton M, Scollay R, Shortman K (1990) Kinetics of mature T-cell development in the thymus. *Proc Natl Acad Sci USA* 87(7):2579–2582.
12. Klein L, Hinterberger M, Wirnsberger G, Kyewski B (2009) Antigen presentation in the thymus for positive selection and central tolerance induction. *Nat Rev Immunol* 9(12): 833–844.
13. Love PE, Bhandoola A (2011) Signal integration and crosstalk during thymocyte migration and emigration. *Nat Rev Immunol* 11(7):469–477.
14. Starr TK, Jameson SC, Hogquist KA (2003) Positive and negative selection of T cells. *Annu Rev Immunol* 21:139–176.
15. Takahama Y (2006) Journey through the thymus: Stromal guides for T-cell development and selection. *Nat Rev Immunol* 6(2):127–135.
16. von Boehmer H, Kisielow P (2006) Negative selection of the T-cell repertoire: Where and when does it occur? *Immunol Rev* 209:284–289.
17. Patel DD, Haynes BF (1993) Cell adhesion molecules involved in intrathymic T cell development. *Semin Immunol* 5(4):282–292.
18. St-Pierre Y, Hugo P, Legault D, Tremblay P, Potworowski EF (1996) Modulation of integrin-mediated intercellular adhesion during the interaction of thymocytes with stromal cells expressing VLA-4 and LFA-1 ligands. *Eur J Immunol* 26(9):2050–2055.
19. Shu F, Holzmann B, Seibold F, Erle D, Kearney JF (2002) Activated alpha4 integrins are preferentially expressed on immature thymocytes and activated T cells. *Dev Immunol* 9(2):73–84.
20. Savino W, Dalmau SR, Dealmeida VC (2000) Role of extracellular matrix-mediated interactions in thymocyte migration. *Dev Immunol* 7(2-4):279–291.
21. Shortman K, Egerton M, Spangrude GJ, Scollay R (1990) The generation and fate of thymocytes. *Semin Immunol* 2(1):3–12.
22. Cambi A, et al. (2006) Organization of the integrin LFA-1 in nanoclusters regulates its activity. *Mol Biol Cell* 17(10):4270–4281.
23. Kucik DF (2002) Rearrangement of integrins in avidity regulation by leukocytes. *Immunol Res* 26(1-3):199–206.
24. Rossy J, Owen DM, Williamson DJ, Yang Z, Gaus K (2013) Conformational states of the kinase Lck regulate clustering in early T cell signaling. *Nat Immunol* 14(1):82–89.
25. Lelek M, et al. (2012) Superresolution imaging of HIV in infected cells with FlAsH-PALM. *Proc Natl Acad Sci USA* 109(22):8564–8569.
26. Chen W, Lou J, Evans EA, Zhu C (2012) Observing force-regulated conformational changes and ligand dissociation from a single integrin on cells. *J Cell Biol* 199(3): 497–512.
27. Chen W, Lou J, Zhu C (2010) Forcing switch from short- to intermediate- and long-lived states of the alphaA domain generates LFA-1/ICAM-1 catch bonds. *J Biol Chem* 285(46):35967–35978.
28. Yago T, et al. (2004) Catch bonds govern adhesion through L-selectin at threshold shear. *J Cell Biol* 166(6):913–923.
29. Liston A, Lesage S, Wilson J, Peltonen L, Goodnow CC (2003) Aire regulates negative selection of organ-specific T cells. *Nat Immunol* 4(4):350–354.
30. Zuklys S, et al. (2000) Normal thymic architecture and negative selection are associated with Aire expression, the gene defective in the autoimmune-polyendocrinopathy-candidiasis-ectodermal dystrophy (APECED). *J Immunol* 165(4):1976–1983.
31. Anderson MS, et al. (2002) Projection of an immunological self shadow within the thymus by the aire protein. *Science* 298(5597):1395–1401.
32. Kurts C, et al. (1996) Constitutive class I-restricted exogenous presentation of self antigens in vivo. *J Exp Med* 184(3):923–930.
33. Robertson JM, Jensen PE, Evavold BD (2000) DO11.10 and OT-II T cells recognize a C-terminal ovalbumin 323-339 epitope. *J Immunol* 164(9):4706–4712.
34. Holl EK, et al. (2011) Plexin-D1 is a novel regulator of germinal centers and humoral immune responses. *J Immunol* 186(10):5603–5611.
35. Marshall BT, et al. (2003) Direct observation of catch bonds involving cell-adhesion molecules. *Nature* 423(6936):190–193.
36. Kong F, García AJ, Mould AP, Humphries MJ, Zhu C (2009) Demonstration of catch bonds between an integrin and its ligand. *J Cell Biol* 185(7):1275–1284.
37. Guo B, Guilford WH (2006) Mechanics of actomyosin bonds in different nucleotide states are tuned to muscle contraction. *Proc Natl Acad Sci USA* 103(26):9844–9849.
38. Yakovenko O, et al. (2008) FimH forms catch bonds that are enhanced by mechanical force due to allosteric regulation. *J Biol Chem* 283(17):11596–11605.
39. Yago T, et al. (2008) Platelet glycoprotein Ibalpha forms catch bonds with human WT vWF but not with type 2B von Willebrand disease vWF. *J Clin Invest* 118(9):3195–3207.
40. Akiyoshi B, et al. (2010) Tension directly stabilizes reconstituted kinetochore-microtubule attachments. *Nature* 468(7323):576–579.
41. Rakshit S, Zhang Y, Manibog K, Shafraz O, Sivasankar S (2012) Ideal, catch, and slip bonds in cadherin adhesion. *Proc Natl Acad Sci USA* 109(46):18815–18820.
42. Lee CY, et al. (2013) Actin depolymerization under force is governed by lysine 113: glutamic acid 195-mediated catch-slip bonds. *Proc Natl Acad Sci USA* 110(13): 5022–5027.
43. Oinuma I, Katoh H, Negishi M (2006) Semaphorin 4D/Plexin-B1-mediated R-Ras GAP activity inhibits cell migration by regulating beta(1) integrin activity. *J Cell Biol* 173(4): 601–613.
44. Janssen BJ, et al. (2010) Structural basis of semaphorin-plexin signalling. *Nature* 467(7319):1118–1122.
45. Nogi T, et al. (2010) Structural basis for semaphorin signalling through the plexin receptor. *Nature* 467(7319):1123–1127.
46. Springer TA, Wang JH (2004) The three-dimensional structure of integrins and their ligands, and conformational regulation of cell adhesion. *Adv Protein Chem* 68:29–63.
47. Lefort CT, et al. (2012) Distinct roles for talin-1 and kindlin-3 in LFA-1 extension and affinity regulation. *Blood* 119(18):4275–4282.
48. Casazza A, et al. (2010) Sema3E-Plexin D1 signaling drives human cancer cell invasiveness and metastatic spreading in mice. *J Clin Invest* 120(8):2684–2698.
49. Liu H, et al. (2010) Structural basis of semaphorin-plexin recognition and viral mimicry from Sema7A and A39R complexes with PlexinC1. *Cell* 142(5):749–761.